ELSEVIER

Surface Science 311 (1994) L649–L654

surface science

Surface Science Letters

# Au(111) reconstruction observed by atomic force microscopy with lateral force detection

H.Y. Nie [1,*], W. Mizutani [1], H. Tokumoto [1]

*Electrotechnical Laboratory, 1-1-4 Umezono, Tsukuba, Ibaraki 305, Japan*

(Received 3 January 1994; accepted for publication 16 February 1994)

**Abstract**

We observed Au(111) $22 \times \sqrt{3}$-like reconstruction by atomic force microscopy with lateral force detection in air. On flat terraces of the gold surface evaporated on mica there appeared the reconstructed patterns as well as atomic lattice image. The lateral force varied across the reconstructed pattern and, in addition, an indication of increasing lateral force at the "elbow" sites of the reconstruction was obtained.

Gold has many advantages over graphite as a substrate for scanning tunneling microscopy (STM) and atomic force microscopy (AFM) of adsorbates, since graphite has some tricky effects, e.g., its steps sometimes generate images resembling DNA or other biological matters [1,2]. The metallic electronic state of gold gives linear current–voltage characteristics, and thus it is easy to identify adsorbates which normally exhibit nonlinear nature. Also the gold surface can be easily modified by self-assembled monolayers and can be functionalized in a controllable manner [3].

There are several ways to prepare gold substrates, such as cleaning of single crystal surface [4], flame annealing of gold wires [5], and vacuum evaporation on mica [6,7]. We adopted the vacuum evaporation method here and optimized the fabrication condition compared with the previous work [6]. The evaporated gold film gives a (111) surface, and with suitable deposition conditions and thermal treatments under high vacuum, the surface forms $22 \times \sqrt{3}$ reconstruction. This structure is known as "herring bone", and has been studied by low energy electron diffraction [7], transmission electron diffraction [8], helium atom diffraction [9], STM in UHV [10,11], and so on. Recently it was found that the structure was observed in air [12] and even in solution [13], where the transition between the $22 \times \sqrt{3}$ and $1 \times 1$ was controlled by the electrochemical potential. Since the unit cell of this reconstruction contains 23 atoms instead of 22, there exists large surface stress [14,15]. (Some papers refer to the reconstruction as $p \times \sqrt{3}$, $p = 22$–$23$.) Extracting one atom from the surface changes the stress fields and therefore results in the pattern modification in large scale [15]. In general, the order of the reconstruction is not perfect but is largely affected by steps and defects on the surface.

* Corresponding author. Fax: +81 298 54 5074.

[1] Present address: National Institute for Advanced Interdisciplinary Research, 1-1-4 Higashi, Tsukuba, Ibaraki 305, Japan.


*SSDI* 0039-6028(94)00108-L

It is reported that metals are deposited selectively at the "elbow" sites of the "herring bone" on the surface [16,17]. This unique effect implies larger interaction at the "elbow" sites, that is, along the reconstructed structure there would be difference in surface energy or sticking coefficient. This difference should be detected by AFM with lateral force detection. Up to now, combined STM/force microscopy, in which the tip position was controlled by the tunneling current and both the compliance and force were detected at the same time [18], showed different compliance along the reconstructed pattern [12]. There were papers reporting AFM images of gold atoms with [13] and without reconstruction [19]. Here we shall present the first report on the AFM observation with lateral force detection of the $22 \times \sqrt{3}$ reconstruction on a gold film.

The mica substrate was cleaved in air and transferred to a deposition chamber, which was evacuated to a pressure down to $5 \times 10^{-9}$ Torr. Then the mica was heated up to 380°C for more than 5 h with a tungsten filament heater from the backside. The pressure before the deposition was $5 \times 10^{-9}$ Torr, and during gold deposition with a speed of 0.5–0.6 nm/s, the pressure was kept below $5 \times 10^{-8}$ Torr. The total thickness measured with a crystal sensor was 200 nm. During and 10 min after the deposition, the mica was kept at 380°C. Then the temperature was lowered gradually and kept at 200°C for about 1 h, and finally cooled to room temperature. The gold film was left in the vacuum for about half a day before it was taken out of the chamber. The temperature was measured with a thermocouple attached to the backside of the substrate.

We used an AFM (Seiko Instruments Inc., SPA300) equipped with a quadrant photodiode system which enables measurements of the lateral force as well as the vertical force. A V-shaped microfabricated cantilever with spring constant of 0.1 N/m was used. The sample was measured within 6 h after removal from the vacuum chamber. We scanned with a constant vertical "attractive" force of 0.4 nN. (The expression "attractive" means here that the total measured force is attractive.) Scanning with a "repulsive" force also exhibited similar results as with "attractive" force.

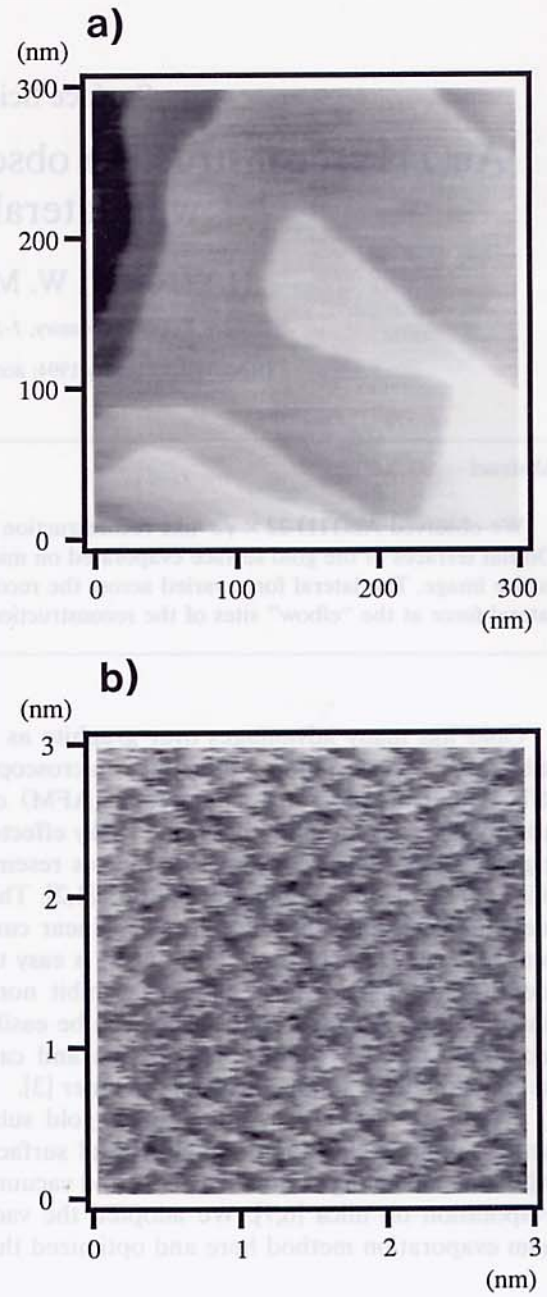


Fig. 1. (a) AFM image of the Au(111) surface. Scanning speed is 3000 nm/s. All the steps are monatomic, i.e., 0.24 nm high. (b) Atomic image of the gold surface. Scanning speed is 120 nm/s. The gray scale of the lateral force is 2 nN.

However, it does not necessarily mean that the force at the tip apex is repulsive or attractive, since there are large nonlocal forces, such as the capillary force, between the tip and surface, especially in air. We can only specify the total force by measuring the bending of the cantilever.

Fig. 1a is a constant force AFM image showing atomically flat gold surface with monatomic steps of about 0.24 nm in height. When zooming in, we obtained "atomic" images on the terraces rather easily with the AFM, though in low magnification images the atoms are smeared out due to the limited sampling. Fig. 1b is a lateral force image taken in the constant vertical force mode, showing a periodic triangular pattern with the same lattice constant as that of the Au(111) surface. The data is displayed without filtering. Simultaneous imaging of the topography and lateral force showed that the topographic corrugation changes in-phase with the lateral force with an amplitude of about 0.1 nm, in agreement with the AFM result by Manne et al. [19]. The lateral force was estimated from the dimensions and material of the cantilever [20] and sensitivity of the detection system by using the formula given by Meyer and Amer [21]. For simplicity, the V-shaped cantilever was assumed to be a rectangular one. The lateral force on the terrace of the gold surface calculated from the friction loop measurement is about 3–4 nN on average, and the corrugation amplitude of the atoms is about 1 nN in this particular case. (Normally we observe a smaller lateral force corrugation of about 0.5 nN, as shown in Fig. 4b.) Suppose that the conventional relation between the vertical force and friction holds in the nanometer scale region, the friction coefficient of about 0.5 yields a vertical force of 6–8 nN. It is reasonable that the detected attractive force of 0.4 nN stems from the difference of this repulsive force of 6–8 nN and almost the same amount of nonlocal attractive force.

The surface reconstruction was observed clearly in lateral force images, because of the larger contrast in the lateral force signal. On the terrace separated by two monatomic steps (A and B) in Fig. 2, there appear clear meandering vertical stripes with a spacing of 7.5–8.0 nm, in good agreement with previous STM and AFM works

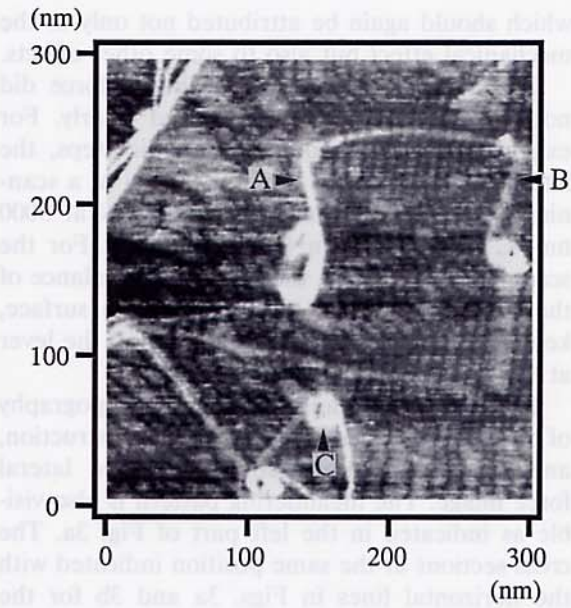


Fig. 2. Lateral force image of the Au(111) surface. The surface is scanned from left to right with a scanning speed of 1500 nm/s. The force increases both at the up-going monatomic step (A), down-going step (B), and hole (C) (see text).

[10–13,15–17]. The scan direction in the image was from left to right with a speed of 1500 nm/s. The same spacing was consistently obtained with different scanning directions, scanning speeds, and the size of scanning areas. Thus, we confirmed that the image was not due to artifacts like noise or pickups from the measuring instrument and the environment.

In the left and lower part of Fig. 2, there are less ordered stripes with wider spacing than observed between A and B. We attribute these regions as partly damaged reconstructions. We will discuss this problem later.

The lateral force increased by 2.7 nN at the up-going step A. At the down-going step B, the force also increased by 1.2 nN, contrary to the prediction assuming only mechanical torque. Therefore, we have to assume some additional reasons, e.g. stronger interaction intrinsic to the steps or adsorbates at the steps mediating the interaction. On the depression C which is 4 nm deep, the lateral force increased by 11.1 nN,

which should again be attributed not only to the mechanical effect but also to some other effects.

The average and change in lateral force did not depend on the scanning speed clearly. For example, at the up-going monatomic steps, the lateral force increased by $4.1 \pm 1.3$ nN at a scanning speed of 1500 nm/s, $4.6 \pm 0.9$ nN at 3000 nm/s, and $3.8 \pm 0.9$ nN at 6000 nm/s. For the scanning speed above, the microscopic balance of the force and torque may hold at the surface, keeping the magnitude of the torsion of the lever at the steps almost unchanged.

Fig. 3a is a constant vertical force topography of one of the terraces showing the reconstruction, and (b) is the simultaneously recorded lateral force image. The meandering pattern is also visible as indicated in the left part of Fig. 3a. The cross sections at the same position indicated with the horizontal lines in Figs. 3a and 3b for the topography and lateral force image are shown in the upper and lower parts of Fig. 3c, respectively. The lateral force changes in-phase with the topography.

At the "elbow" sites where the reconstructed pattern changes direction indicated by the arrows in Fig. 3a, the lateral force is larger by about 1 nN shown as white horizontal stripes in Fig. 3b, indicating the larger interaction between the tip and surface. This interaction may be caused either directly by the intrinsic surface property as observed in UHV [16,17], or indirectly by the adsorbates covering the site more strongly due to the intrinsic interaction.

The reconstruction disappears normally half a day after the gold is exposed to air, probably because some kind of contaminant on the surface may change the surface energy. Since the reconstruction is realized under a delicate energy balance at the surface [14], some adsorbates could change the surface energy and destroy the reconstruction [13].

The reconstruction is also not robust against the continuous scanning. We noticed that in some cases the reconstruction was damaged after scanning. This makes imaging the atoms and the reconstruction at the same time difficult. Since scanning area sizes suitable to image the atomic lattice and the reconstruction differ by about a factor 20, we have to use the condition which is not optimum for both, and after adjusting the observation condition, the reconstruction is usually damaged to some extent. Thus, we obtained only images with faint contrast, one of which is

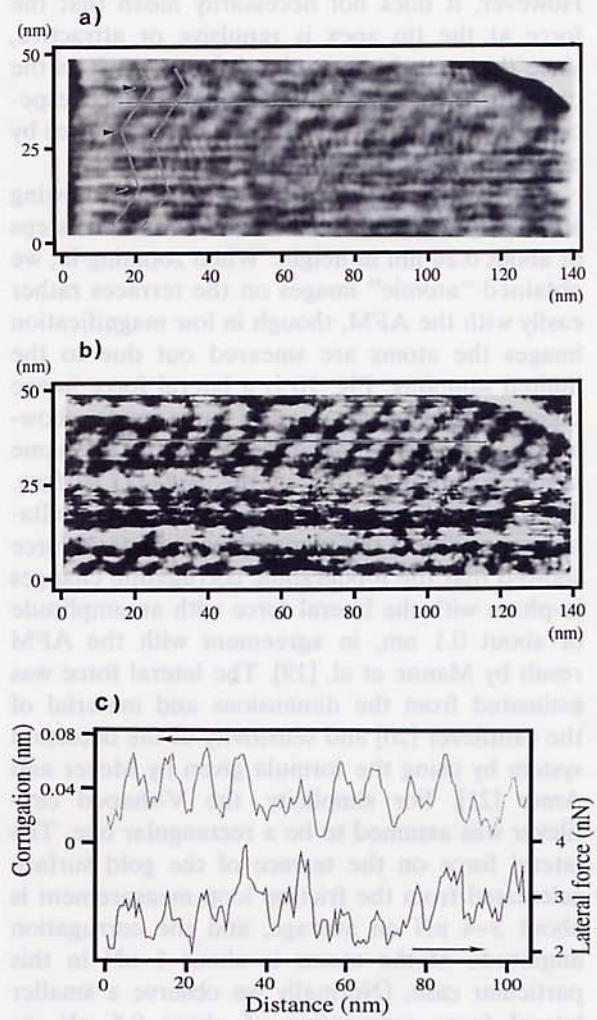


Fig. 3. The $22 \times \sqrt{3}$ reconstruction of the Au(111) surface. (a) Constant force topography. Scanning speed is 1200 nm/s. In the left part, the reconstruction is highlighted with guide lines, and the elbow sites are marked with arrows. (b) Lateral force image taken simultaneously with (a). (c) Cross sections at the same position as indicated by the horizontal lines in (a) and (b). The measured spacing is about 10 nm, larger than the theoretical spacing of 7.5 nm, partly because the cross section is not perpendicular to the reconstructed pattern, and partly because of the disorder of the reconstruction.

filtered to enhance the atomic lattice and is shown in Fig. 4a. The inset shows the two-dimensional Fourier transform of the original data showing the periodicity of the atoms clearly. The cross section across the reconstruction (Fig. 4b) shows the double-ridge structure with the 23 atoms, like the UHV STM studies [15–17] and theoretical calculation [14], although the reconstruction here is about to collapse and becoming wider on both side.

Before deducing conclusions from the present results, we shall check out the "cross talk" between vertical and lateral components of the force due to the detection system. The ratio of corrugation amplitudes in the topography and the lateral force differs in the case of the atomic image (Fig. 1b), the steps and holes (Fig. 2), and the reconstruction (Fig. 3). A careful comparison between the upper and lower parts in Fig. 3c shows that the lateral force changes in-phase with the topography but its magnitude is not proportional to the topographic corrugation amplitude. Therefore, we believe that the measured changes in the lateral force reflect the surface properties other than topography.

In conclusion, we observed the $22 \times \sqrt{3}$ reconstruction of an Au(111) surface by AFM with lateral force detection in air for the first time. The corrugation amplitudes of the topography were about 0.1 nm for the atoms and 0.04 nm for the reconstruction. The average friction force on the gold terrace was estimated to be 3–4 nN on average under our experimental conditions. The corrugation amplitudes of the lateral force were about 0.5 nN for the atoms, and 1 nN for the reconstruction. The lateral force changed across the reconstructed pattern, and increased at the "elbow" sites.

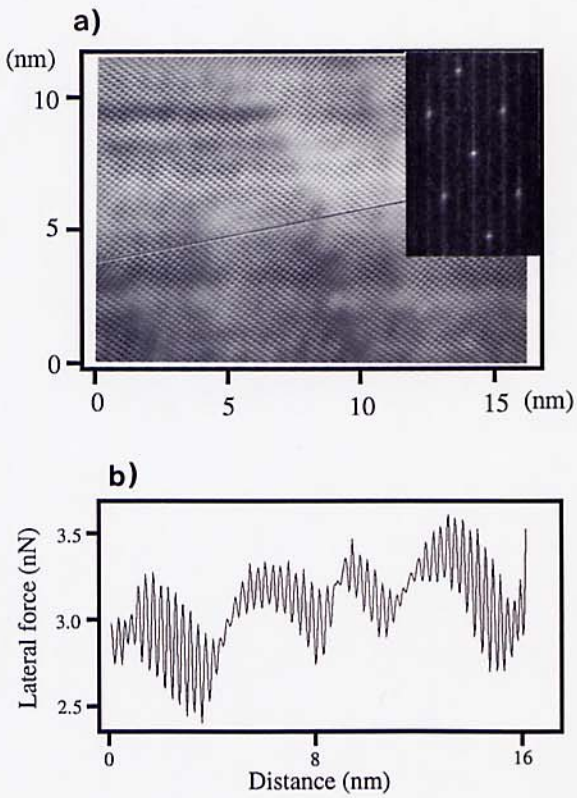


Fig. 4. Lateral force image of atomic lattice and reconstructed pattern. (a) Filtered image; inset: spectrum of the raw data, showing atomic periodicity. (b) Cross section along the line in (a).

We thank T. Shimizu for his valuable discussion on AFM measurement. One of us (H.Y.N.) acknowledges financial support from Science and Technology Agency of Japan.

## References

[1] C. Clemmer and T. Beebe, Jr., Science 251 (1991) 640.
[2] W. Heckl and G. Binnig, Ultramicroscopy 42–44 (1992) 1073.
[3] L. Häussling, B. Michel, H. Ringsdorf and H. Rohrer, Angew. Chem. Int. Engl. 30 (1991) 569.
[4] R. Jaklevic and L. Elie, Phys. Rev. Lett. 60 (1988) 120.
[5] J. Schneir, R. Sonnenfeld, O. Mariti and P. Hansma, J. Appl. Phys. 63 (1988) 717.
[6] J. Inukai, W. Mizutani, K. Saito, H. Shimizu and Y. Iwasawa, Jpn. J. Appl. Phys. 30 (1991) 3496.
[7] M. Van Hove, R. Koestner, P. Stair, J. Biberian, L. Kesmodel, I. Bartos and G. Somorjai, Surf. Sci. 103 (1981) 189.
[8] Y. Tanishiro, H. Kanamori, K. Takayanagi, K. Yagi and G. Honjo, Surf. Sci. 111 (1981) 395.
[9] U. Harten, A. Lahee, J. Toennies and Ch. Wöll, Phys. Rev. Lett. 54 (1985) 2619.
[10] Ch. Wöll, S. Chiang, R. Wilson and P. Lippel, Phys. Rev. B 39 (1989) 7988.

[11] M. Doveck, C. Lang, J. Nogami and C. Quate, Phys. Rev. B 40 (1989) 11973.
[12] D. Anselmetti, private communication.
[13] P. Oden, N. Tao and S. Lindsay, J. Vac. Sci. Technol. B 11 (1993) 137.
[14] S. Narasimhan and D. Vanderbilt, Phys. Rev. Lett. 69 (1992) 1564; 69 (1992) 2455.
[15] Y. Hasegawa and Ph. Avouris, Science 258 (1992) 1763.
[16] D. Chambliss, R. Wilson and S. Chiang, Phys. Rev. Lett. 66 (1991) 1721.
[17] J. Strocio, D. Pierce, R. Dragoset and P. First, J. Vac. Sci. Technol. A 10 (1992) 1981.
[18] D. Anselmetti, Ch. Gerber, B. Michel, H. Güntherodt and H. Rohrer, Rev. Sci. Instrum. 63 (1992) 3003.
[19] S. Manne, H. Butt, S. Gould and P. Hansma, Appl. Phys. Lett. 56 (1990) 1758.
[20] We used "Olympus microcantilevers", whose detailed information was supplied from A. Toda.
[21] G. Meyer and N. Amer, Appl. Phys. Lett. 57 (1990) 2089.